A model for the nucleation of diamond clusters on Si(111) substrates

Pushpa Mahalingam, Huimin Liu,[a] and David S. Dandy[b]
Department of Chemical Engineering, Colorado State University, Fort Collins, Colorado 80523

(Received 9 August 1996; accepted for publication 1 November 1996)

A theoretical study of the nucleation, size, and structure of diamond phase carbon clusters on Si(111) substrates is presented. Molecular mechanics analysis has been utilized to predict energetically and entropically feasible pathways for nucleation of the carbon clusters. Several mechanistic pathways for nucleation of carbon clusters are examined with CH_3 and/or C_2H_2 as the nucleation precursors. A possible model for the nucleation mechanism of diamond-phase carbon clusters on the β-SiC(111) surface, which forms epitaxially on Si(111) substrates, is presented. The critical size of the carbon clusters is computed based on the atomistic theory of nucleation and the proposed nucleation mechanisms. © *1997 American Institute of Physics.* [S0021-8979(97)09403-6]

INTRODUCTION

The synthesis of thin diamond films using a variety of chemical vapor deposition (CVD) methods has received significant attention in recent years, primarily because the unique properties of diamond make it an attractive candidate for a wide range of applications, such as semiconductor devices, cutting and grinding tools, and windows for visible and infrared transmission.[1] Nucleation and growth processes of diamond films have become subjects of intensive study in an effort to enhance diamond nucleation and control film morphology during the CVD processes.[2–7]

In most chemical vapor deposition methods, diamond nucleation on non-diamond surfaces without pretreatment is usually difficult and slow. One of the more commonly used techniques for enhancing the nucleation of diamond is by scratching the substrate surface with either hard abrasives or a paste of fine diamond particles.[1] Diamond nucleation on non-diamond substrates occurs most often on an intermediate layer of materials such as metal carbides, graphite, amorphous, or diamond-like carbon (DLC) formed at the substrate surface due to chemical interactions between activated gas species and the substrate during the incubation period.[8–11] It has been shown that, in the early stages of the growth of diamond by microwave plasma CVD (MPCVD) and hot filament CVD (HFCVD),[12–15] an intermediate carbide layer is formed on silicon substrates. For example, Kobayashi *et al.*[16] have reported that a 2 nm thick intermediate amorphous layer on a silicon substrate was observed for films grown via an electron-assisted CVD method. Joffreau *et al.*[17] performed a systematic study of diamond growth on refractory metals (all carbide formers) and observed that diamond nucleation occurred only after the formation of a thin carbide layer. Other non-carbide carbonaceous nucleation promoters like graphite[18] and DLC[19] have been postulated to exist as well during the early stages of diamond CVD. Diamond-like carbon is a non-crystalline, hard, carbonaceous film whose atom number density is significantly greater than other amorphous carbon and hydrocarbon solids of the same elemental composition, but always less than that of diamond.

Stoner *et al.*[20] concluded that carbide formation may only play an intermediate or secondary role in diamond nucleation and that there exists an intermediate nucleation step between the carbide formation and actual diamond nucleation. They observed excess carbon on the surface of β-SiC and hypothesized that the surface carbon contributed significantly to the nucleation of diamond and that the β-SiC layer acts as a temporary, but critical, host on which the carbon can accumulate until clusters of the appropriate size and structure required for diamond nucleation develop. A separate study by McGinnis *et al.*,[21] which examined the role of carbon in nucleation, indicates that a specific configuration of carbon on the substrate appears to be responsible for heterogeneous nucleation of diamond. They suggest two possibilities for this configuration: (1) a carbon form, such as DLC, similar enough to diamond for nucleation to occur, or (2) an actual diamond-phase cluster. It has been postulated by Badziag *et al.*[22] that the critical carbon configuration consists of small diamond-phase clusters, since the formation of very small carbon clusters which are hydrogen terminated may be more thermodynamically stable under deposition conditions as diamond rather than as graphite or DLC. This suggestion is consistent with the observations by George *et al.*[23] of a small cluster-like precursor layer seen by atomic force microscopy (AFM) imaging, which showed the heterogeneous nucleation of ordered diamond crystallites. No information about the size or structure of the diamond crystallites was stated in the work by George *et al.* To date, the information about the size, structure, and chemistry of diamond clusters or nuclei is primarily speculative.

Silicon is a common substrate material for diamond deposition.[1] Heteroepitaxial nucleation of diamond on silicon wafers may take place through the formation of the intermediate β-SiC epitaxial conversion layer on the surface of silicon due to the crystallographic registry across the interface.[24,25] Epitaxial nucleation of diamond on Si(100) wafers has been demonstrated to occur via the formation of an epitaxial β-SiC conversion layer that formed during the *in situ* carburization step.[26] The β-SiC(111) layer is known to form as an intermediate layer on the Si(111) substrate due to the epitaxial relationship between silicon and β-SiC. In the

[a]Present address: Concurrent Technologies Corp., Johnstown, PA 15904
[b]Electronic mail: dandy@engr.colostate.edu

 0021-8979/97/81(4)/1966/12/$10.00

present work, several mechanisms for the nucleation of diamond-phase carbon clusters on β-SiC(111) are examined. The β-SiC(111) surface is assumed to be hydrogenated and therefore, in an unreconstructed state. The critical size and structure of the diamond phase carbon clusters formed on β-SiC is computed based on the proposed nucleation mechanism. The diamond-phase carbon clusters become thermodynamically stable after they reach a specific size, referred to as the critical cluster size (CCS), and this quantity is predicted using atomistic nucleation theory. The etch-resistant, stable diamond-phase clusters may subsequently serve as nucleation centers or seeds for the growth of continuous diamond films by providing necessary sites for diamond nucleation.

In this work, energetically and entropically favorable pathways leading to the nucleation of diamond-phase carbon clusters are predicted using molecular mechanics. Subsequently, the critical cluster size of the carbon clusters is calculated based on the feasible nucleation mechanisms of carbon clusters. The theoretical method employed in the current calculations is presented below.

THEORETICAL METHOD

The β-SiC(111) surface is assumed to be hydrogenated and therefore unreconstructed during typical diamond CVD conditions due to the presence of excess atomic hydrogen. To analyze the stability of clusters on β-SiC(111), the molecular mechanics method developed by Allinger and coworkers, MM3,[27] has been applied to examine the hydrogenated surface of β-SiC. Periodic boundary conditions are incorporated into the computational algorithm, permitting calculations comparable in size to modest-sized clusters but without complications from edge effects. The 1992 version of the force field, MM3(92),[28,29] with parameters for saturated, unsaturated, conjugated hydrocarbons, and silicon atoms is accurate to within $\sim\pm 0.1$ Å in bond length, $\pm 1°$ in bond angle between atoms other than hydrogen, and $\pm 4°$ in torsional angles. Calculated heats of formation for a wide variety of hydrocarbon compounds are consistently within chemical accuracy, that is, ± 1 kcal/mol. The force field is successful in modeling not only small, simple molecules, but also large molecules and some highly strained molecules.[28]

The MM3 force field for molecules may be summarized as

$$E=\Sigma E_s+\Sigma E_\theta+\Sigma E_\omega+\Sigma E_{s\theta}+\Sigma E_{\omega s}+\Sigma E_{\theta\theta'}+\Sigma E_{vdw}+\Sigma E_{dpl}, \quad (1)$$

such that the total energy E is assumed to be the linear combination of different atom interaction energies: E_s the bond stretching energy, E_θ the angle bending energy, E_ω the torsional energy, $E_{s\theta}$ the stretch-bend energy, $E_{\omega s}$ the torsion stretch energy, $E_{\theta\theta'}$ the bend coupling energy, E_{vdw} the van der Waals interaction energy between two atoms which are bonded neither to each other nor to a common atom, and E_{dpl} the dipole interaction energy. In Eq. (1), the summations extend over all the bonds, bond angles, torsion angles, and non-bonded interactions between atoms not bound to each other or to a common atom. The specific equations and associated parameters used to calculate each energy term can be found in the literature.[27,28]

Heats of formation are calculated using[27,29]

$$\Delta H_f=\Delta H_{bond}+\Delta H_{struct}+\Delta H_{steric}+\Delta H_{thermo}, \quad (2)$$

where ΔH_{bond} is the sum of the bond energy contributions, ΔH_{struct} is the sum of structural energy contributions for functional groups such as methyl groups or five-membered rings, ΔH_{steric} is the steric energy resulting from Eq. (1) after minimization, and ΔH_{thermo} is the partition function contribution. For hydrocarbons and silicon, ΔH_{thermo} is 2.4 kcal/mol (to account for translation, rotation, and a correction for constant volume), and for alkanes in particular, an extra torsional correction of 0.4 kcal/mol is added for each bond about which there is a rotational barrier of less than 7 kcal/mol. Because the surface species considered here have neither translational nor rotational degrees of freedom, ΔH_{thermo} is not considered.

The slab chosen for the hydrogenated β-SiC(111) is 4 layers thick and consists of 5×5 unit cells, with a total of 99 carbon atoms, 99 silicon atoms, and 126 hydrogen atoms. In order to ensure that the computed results were not dependent on the size of the slab, calculations have been carried out for two of the molecules, using a larger slab, 7 layers thick consisting of 8×8 unit cells, with a total of 447 carbon atoms, 447 silicon atoms, and 350 hydrogen atoms. The predicted thermodynamic properties for the larger structures were within 0.4% of those predicted for the smaller slab.

The formation of carbon clusters are assumed to occur through the combination of methyl radicals, acetylene molecules, and hydrogen atoms because these are typically the major species contributing to diamond nucleation and growth in diamond CVD processes.[31,32] In the calculations, methyl radicals are assumed to preferentially chemisorb on the silicon atoms. The results of a study by Ohshita[33] indicate that the chemisorption energy of a CH_2 radical on a silicon atom is greater than that on a carbon atom during the β-SiC vapor phase epitaxial growth under conditions very similar to that existing during diamond CVD.

To model the characteristics of a solid slab, the bottom layer of substrate atoms are fixed in position during the calculations, preventing expansion or contraction of the unit cell in all directions. The Cartesian coordinates of the carbon and silicon atoms are defined with respect to their ideal positions in the bulk, as determined by simple geometry using β-SiC lattice constant of 4.35 Å.[30] A full Newton–Raphson energy minimization is done for each calculation. The eigenvalues of the Hessian matrix are checked to ensure that a true energy minimum is reached, rather than an intermediate transition state.

By calculating the heats of reaction and Gibbs energy of reaction between methyl radicals, acetylene molecules, atomic hydrogen and various surface complexes, a sequence of energetically and entropically feasible reactions leading to the nucleation of diamond-phase carbon clusters are proposed. It has been reported that C_2H_2 and CH_3 are the dominant growth species during diamond CVD.[34,35] Several mechanistic paths have been examined, including (i) the for-

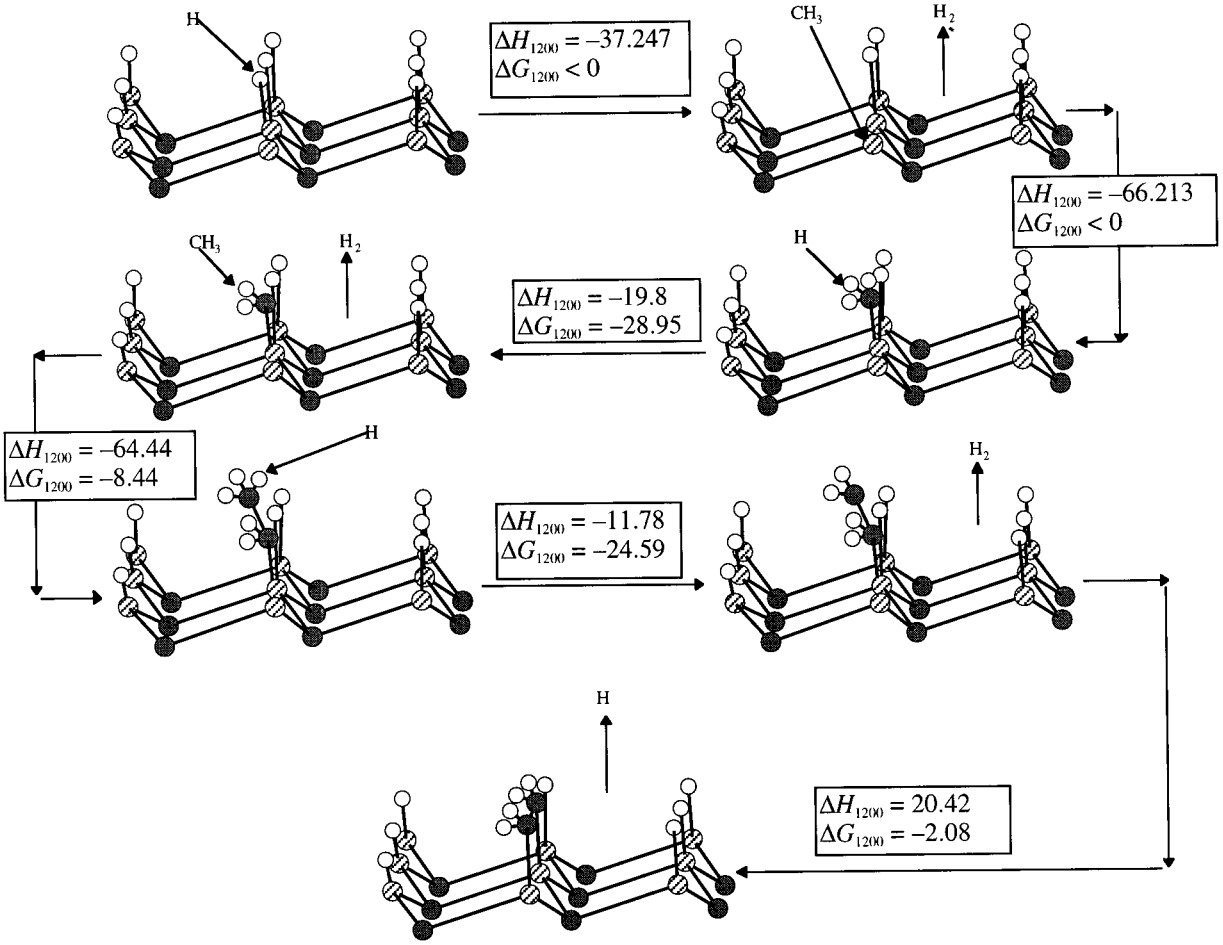

FIG. 1. First route for the nucleation of diamond phase carbon cluster using CH_3 as the precursor species. ΔH_{1200} and ΔG_{1200} are in kcal/mol. (●): C atom, (⊘): Si atom, (○): H atom. Bond lengths not to scale.

mation of clusters from CH_3 radicals alone, and (ii) the formation of clusters with C_2H_2 and CH_3 as nucleation precursors. The heats of reaction, ΔH_T, and the Gibbs energy of reaction, ΔG_T, are calculated for each elementary reaction at three different temperatures, $T=298$ K, 1000 K, and 1200 K. The heat of reaction is only weakly temperature dependent, although the free energy change of reaction does depend strongly on temperature. Because typical gas-phase temperatures above substrate surface during diamond CVD are approximately 1200 K, for reference, the values of ΔH_{1200} and ΔG_{1200} are given alongside each reaction in the Figs. (1)–(3) and Tables I and II.

RESULTS AND DISCUSSION

Several mechanistic paths for nucleation of carbon clusters are examined in this section. The heats of reaction, ΔH_T, and the Gibbs energy of reaction, ΔG_T, for each elementary reaction in each path for nucleation of diamond-phase carbon cluster is calculated utilizing MM3.

The heat of reaction for the gas-phase reaction

$$CH_4+H \Leftrightarrow CH_3+H_2 \quad \Delta H_{298}=0.53 \text{ kcal/mol} \tag{3}$$

is computed from the heat of formation of CH_4, CH_3, H_2, and H.[36] Although the heat of reaction (3) is positive, this reaction will occur due to the abundance of H atoms during diamond CVD.

The binding energy of a H atom on a Si(111) surface is 69.293 kcal/mol of H atoms.[37] Therefore, the removal of a H atom from a Si surface atom may be represented by the reaction:

$$SiH(s) \Leftrightarrow Si\bullet(s)+H \quad \Delta H_{298}=69.3 \text{ kcal/mol}, \tag{4}$$

where Si• is a surface radical site. The heat of formation of two H atoms is known to be 104.2 kcal/mol:[38]

$$H_2 \Leftrightarrow H+H \quad \Delta H_{298}=104.2 \text{ kcal/mol}. \tag{5}$$

Using the heats of reaction of (4) and (5), the heat of formation of silicon radicals can be computed.

CH_3 MECHANISM

There are three principal routes for the nucleation of a propane-like kernel (a term first used by Frenklach *et al.*[39,40]) using CH_3 alone as the nucleation precursor. The propane-like kernel is the seed for the growth of a new diamond phase

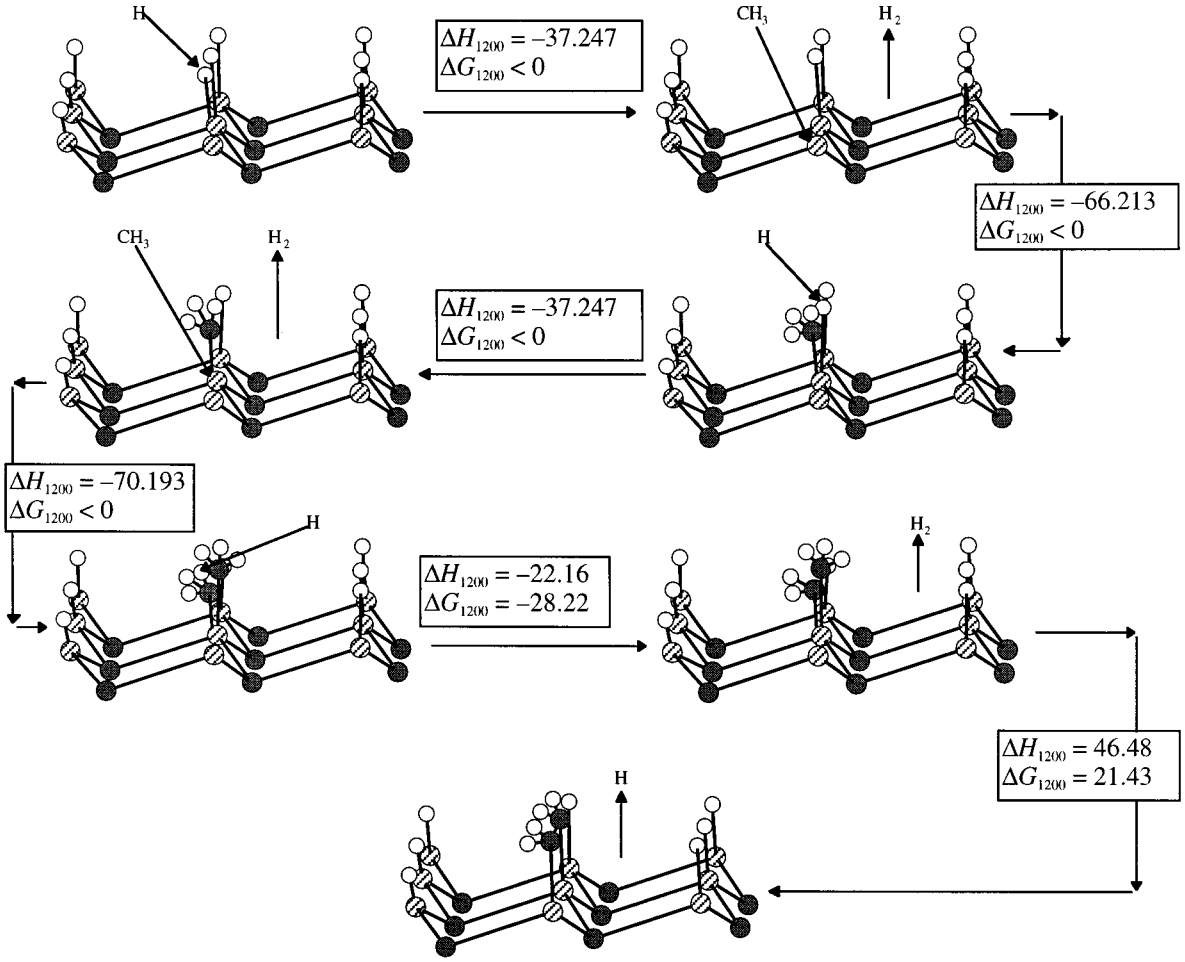

FIG. 2. Second route for the nucleation of diamond phase carbon clusters using CH_3 as the nucleation precursor. ΔH_{1200} and ΔG_{1200} are in kcal/mol. (●): C atom, (⊘): Si atom, (○): H atom. Bond lengths not to scale.

carbon cluster. The first route for a methyl based ion-free reaction pathway leading to the nucleation of a propane-like kernel is described by the six step reaction sequence in Table I. In reactions (I.1–I.6) in Table I, the calculated heat of reaction, ΔH_{1200}, and Gibbs energy of reaction, ΔG_{1200} are listed with each reaction. The reactions listed in Table I are illustrated in Fig. 1.

In the reaction sequence listed in Table I, the hydrogenated β-SiC surface is activated by the H abstraction (reaction I.1) forming a surface radical, Si•(s), to which a free methyl radical is added (reaction I.2). The surface complex formed in this manner, $SiCH_3$(s), is activated by H abstraction (reaction I.3), and another free methyl radical is added (reaction I.4). The surface complex, $SiCH_2CH_3$(s), forms a product surface complex, $SiCH_2CH_2Si$(s), through the abstraction of a hydrogen atom from the terminal carbon atom (reaction I.5) and formation of C–Si bond between the created radical and a neighboring surface silicon site, SiH(s) (reaction I.6). The above reaction sequence is illustrated in Fig. 1. Reaction (I.6) is not feasible because it has a positive ΔH although ΔG is negative and hence, is not a likely route for nucleation of diamond clusters. The free energy of reaction (I.1) is likely to be negative since the free energy change of a corresponding reaction for the abstraction of a H atom from a hydrogenated diamond surface by a hydrogen atom is very negative.[39–41] Similarly, the abstraction of a H atom from a hydrogenated silicon site by a gas-phase H atom is likely to be negative because the free energy of a H atom is strongly positive. Such activation reactions are known to proceed spontaneously. The free energy of reaction (I.2) is likely to be negative because it is a radical-radical reaction and such reactions are known to be spontaneous.

The second possible route for a methyl-based reaction sequence forming the surface complex $SiCH_2CH_2Si(s)$ is listed in Table II. This reaction sequence is similar to (I.1)–(I.6) because it also proceeds through H abstractions followed by the CH_3 addition. However, instead of progressing via sequential surface complexes built at the same surface silicon site, it requires the formation of two separate CH_3 adducts at adjacent surface silicon sites (II.1)–(II.2) and (II.3)–(II.4), as shown in Fig. 2. Once the two adducts form, following a H abstraction, reaction (II.5), a C–C bond is formed between the two CH_3 admolecules thereby transforming the surface complex into the product surface complex $SiCH_2CH_2Si$(s) (reaction II.6). The enthalpy and free energy changes for reaction (II.6) are both positive, indicating that this reaction is not a preferred path for the nucleation of the diamond phase clusters.

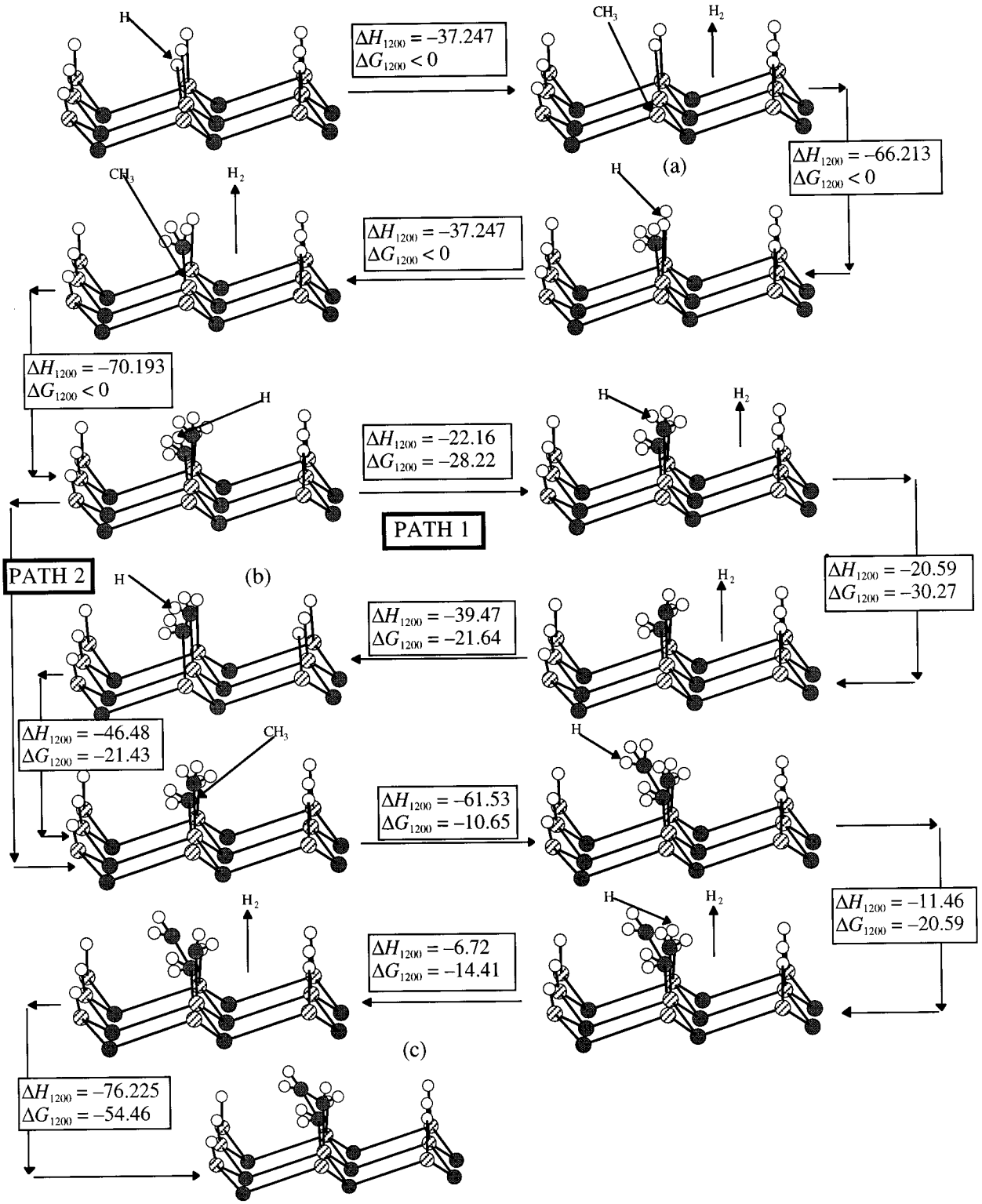

FIG. 3. Third route for the nucleation of diamond clusters using CH_3 as the precursor species. ΔH_{1200} and ΔG_{1200} are in kcal/mol. (●): C atom, (⊘): Si atom, (○): H atom. Bond lengths not to scale.

The third route for a methyl-based reaction sequence involves the creation of the surface complex $SiCH_2CH_2Si(s)$ through the diradical species

$$SiCH_3(s)+H \Leftrightarrow SiCH_2\bullet(s)+H_2 \quad \Delta H_{1200}=-20.6 \text{ kcal/mol}, \tag{6}$$

followed by a radical-radical surface addition reaction:

$$SiCH_2\bullet(s)+SiCH_2\bullet(s) \Leftrightarrow SiCH_2CH_2Si(s)$$

$$\Delta H_{1200}=-39.5 \text{ kcal/mol}. \tag{7}$$

This route is illustrated in Fig. 3. Values for ΔH_{1200} and ΔG_{1200} are listed with each reaction in Fig. 3. The results indicate that reaction (7) has a negative heat of reaction and a negative free energy change of reaction, as expected for a radical-radical reaction. Therefore, the surface complex, $SiCH_2CH_2Si(s)$, could in principle be formed by reaction (7).

TABLE I. First route for the CH_3 based reaction sequence.

Reaction No.	Reaction	ΔH_{1200} (kcal/mol)	ΔG_{1200} (kcal/mol)
1	$SiH(s)+H \Leftrightarrow Si\cdot(s)+H_2$	−37.247	<0
2	$Si\cdot(s)+CH_3 \Leftrightarrow SiCH_3(s)$	−66.213	<0
3	$SiCH_3(s)+H \Leftrightarrow SiCH_2\cdot(s)+H_2$	−19.8	−28.95
4	$SiCH_2\cdot(s)+CH_3 \Leftrightarrow SiCH_2CH_3(s)$	−64.44	−8.44
5	$SiCH_2CH_3(s)+H \Leftrightarrow SiCH_2CH_2\cdot(s)+H_2$	−11.78	−24.59
6	$SiCH_2CH_2\cdot(s)+SiH(s) \Leftrightarrow SiCH_2CH_2Si(s)+H$	20.42	−2.08

The propane-like kernel can then be formed from $SiCH_2CH_2Si(s)$, by the following sequence of reactions:

$$SiCH_2CH_2Si(s)+H \Leftrightarrow SiCH_2\bullet(s)+SiCH_3(s)$$
$$\Delta H_{1200} = -46.5 \text{ kcal/mol},$$
$$\Delta G_{1200} = -21.4 \text{ kcal/mol}, \quad (8)$$

$$SiCH_2\bullet(s)+SiCH_3(s)+CH_3 \Leftrightarrow SiCH_2CH_3(s)+SiCH_3(s)$$
$$\Delta H_{1200} = -61.5 \text{ kcal/mol},$$
$$\Delta G_{1200} = -10.7 \text{ kcal/mol}. \quad (9)$$

In reaction (8), instead of H attacking the structure $SiCH_2CH_2Si(s)$, CH_3 atoms may attack it. In this case the reaction sequence would be as follows:

$$SiCH_2CH_2Si(s)+CH_3 \Leftrightarrow SiCH_2CH_3(s)+SiCH_2\bullet(s)$$
$$\Delta H_{1200} = -24.1 \text{ kcal/mol}, \quad \Delta G_{1200} = 10.6 \text{ kcal/mol}, \quad (10)$$

$$SiCH_2CH_3(s)+SiCH_2\bullet(s)+H \Leftrightarrow SiCH_2CH_3(s)+SiCH_3(s)$$
$$\Delta H_{1200} = -83.9 \text{ kcal/mol},$$
$$\Delta G_{1200} = -42.7 \text{ kcal/mol}. \quad (11)$$

The Gibbs energy change of (10) is positive, which indicates that the rate of the reverse reaction is faster than the forward reaction. Hence, reactions (8) and (9) are predicted to be more favorable than reactions (10) and (11).

Once the product structure, $SiCH_2CH_3(s)$, is formed by reaction (9), a propane-like kernel can be formed by the following reactions:

$$SiCH_2CH_3(s)+SiCH_3(s)+H \Leftrightarrow SiCH_2CH_2\bullet(s)+SiCH_3(s)+H_2$$
$$\Delta H_{1200} = -11.5 \text{ kcal/mol}, \quad (12)$$

TABLE II. Second route for CH_3 based reaction sequence.

Reaction No.	Reaction	ΔH_{1200} (kcal/mol)	ΔG_{1200} (kcal/mol)
1	$SiH(s)+H \Leftrightarrow Si\cdot(s)+H_2$	−37.247	<0
2	$Si\cdot(s)+CH_3 \Leftrightarrow SiCH_3(s)$	−66.213	<0
3	$SiH(s)+H \Leftrightarrow Si\cdot(s)+H_2$	−37.247	<0
4	$Si\cdot(s)+CH_3 \Leftrightarrow SiCH_3(s)$	−70.193	<0
5	$SiCH_3(s)+H \Leftrightarrow SiCH_2\cdot(s)+H_2$	−22.16	−28.22
6	$SiCH_2\cdot(s)+SiCH_3(s) \Leftrightarrow SiCH_2CH_2Si(s)+H$	46.48	21.43

$$SiCH_2CH_2\bullet(s)+SiCH_3(s)+H \Leftrightarrow SiCH_2CH_2\bullet(s)+SiCH_2\bullet(s)+H_2$$
$$\Delta H_{1200} = -6.7 \text{ kcal/mol}, \quad (13)$$

$$SiCH_2CH_2\bullet(s)+SiCH_2\bullet(s) \Leftrightarrow SiCH_2CH_2CH_2Si(s)$$
$$\Delta H_{1200} = -76.3 \text{ kcal/mol}. \quad (14)$$

The propane-like kernel, $SiCH_2CH_2CH_2Si(s)$, may be formed from structure $SiCH_2CH_2Si(s)$ by H atom addition [reaction (8)], CH_3 addition [reaction (9)], H atom abstractions [reactions (12) and (13)], followed by the radical-radical surface reaction (14); this reaction sequence is henceforth referred to as path 1. Another possible mechanism for the formation of the propane-like kernel is by bypassing structure $SiCH_2CH_2Si(s)$, i.e., by reactions in the sequence (II.1), (II.2), (II.3), (II.4), (II.5), (9), (12)-(14), henceforth referred to as path 2. The two paths are illustrated in Fig. 3.

Thus, the third nucleation route via path 1 or path 2 (see Fig. 3) involving the radical-radical surface addition reaction is a very likely mechanism for the nucleation of a diamond-phase carbon cluster. Counteracting the favorable energetics and entropy is the requirement for high selectivity of the gaseous species' attacks on the surface sites, i.e., selective additions of methyl radicals to selectively created adjacent surface radical sites (if CH_3 is supplied by the gas phase), or selective migration of CH_3 radicals to adjacent surface radical sites (if CH_3 is available by surface diffusion after adsorption on the surface) followed by selective abstractions of hydrogen atoms from the formed CH_3 admolecules. Huang *et al.*,[41] using the results from a kinetic study,[42] have estimated that the rate of attack of gaseous species on a neighboring surface site should be lowered by roughly one order of magnitude due to steric selectivity. The low overall rate of nucleation of the diamond phase cluster, due to the steric selectivity of the probable nucleation mechanism suggested above, may explain the large incubation period observed during the early stages of nucleation of diamond films.[1]

The results presented above for nucleation of a propane-like kernel using CH_3 as the precursor species, are qualitatively similar to the computed results predicted for diamond(111) homoepitaxial growth by Huang *et al.*[41] The heat of reaction (I.1) is indicative of the CH_3 chemisorption energy on silicon surface and appears reasonable compared to the CH_2 adsorption energy calculated by Ohshita[33] on a silicon atom.

C_2H_2 AND CH_3 MECHANISM

Acetylene has been identified as a stable product in a diamond CVD environment, and it has been shown that C_2H_2 and CH_3 are the most likely species available for the extension of the diamond lattice.[34,35] Because C_2H_2 is a potential stable growth species in diamond CVD, the nucleation of diamond-phase clusters, using both C_2H_2 and CH_3 as the nucleation precursors, is examined in this work. Three different nucleation sequence routes have been investigated in this work using different combinations of the CH_3 and C_2H_2 addition, plus hydrogen abstraction and termination. The first two of these routes are based on a growth mechanism proposed by Frenklach *et al.*[39,40] for diamond growth on a step

fragment on the (111) plane of a diamond surface, using acetylene as the main monomer growth species. The first nucleation route was not plausible due to the positive free energy changes and positive heats of key reactions while the second nucleation sequence was found to be thermodynamically unfavorable due to positive free energy changes for key reactions; the results found here for this general growth mechanism are consistent with those from a previous investigation.[43]

The third route for the nucleation of diamond phase clusters using C_2H_2 and CH_3 forms new segments of the diamond structure in the same row, rather than in adjacent rows as considered in the first two sequences. As with the second sequence, ΔG was found to be positive for key reactions involving C_2H_2 addition, once again indicating that other nucleation routes may be favored. Although all reactions considered in the second and third nucleation sequences are exothermic, a large negative entropy change in C_2H_2 addition reactions may prevent the nucleation mechanisms by C_2H_2 and CH_3 from occurring. However, the nucleation route using CH_3 alone as the nucleation precursor is energetically and entropically feasible. Therefore, it may be concluded that the nucleation mechanism using CH_3 as the precursor will be favored over the nucleation mechanism using C_2H_2 and CH_3 as the combined precursors.

CRITICAL CLUSTER SIZE

The critical cluster size (CCS), n_0, is defined as a measure of thermodynamic stability such that clusters with fewer than n_0 atoms will dissociate, whereas clusters with more than n_0 atoms are stable. There are two approaches to analyze nucleation, classical, and atomistic (non-classical). In the atomistic approach to nucleation theory, the critical size is defined using the concepts of statistical mechanics, whereas in the classical approach bulk material parameters are used to describe the clusters. Since deposition from the gas phase occurs under high supersaturation, small critical clusters are expected to form during the heterogeneous nucleation of diamond by CVD. It has been pointed out in the literature that the predictions of the classical theory are far less reliable for heterogeneous than for homogeneous nucleation.[44] A microscopic description, in which no assumptions are made regarding the shape or size of the clusters, is therefore preferable for theoretical predictions regarding nucleation on surfaces. In this work, the CCS for a Si(111) substrate, is evaluated based on the nucleation mechanisms for the diamond-phase clusters proposed before in this work. An important assumption is that the desorption of entire clusters is not considered in this work when computing the critical cluster size.

The Gibbs energy of formation of a cluster of n atoms is defined in the atomistic approach as[45]

$$G_n = nkT_s \ln\left(\frac{\nu_0}{J}\right) - (E_n + nE_a), \tag{15}$$

where E_n is the binding energy of a cluster of n atoms and E_a is the single atom adsorption energy, k is Boltzmann's constant, T_s is the substrate temperature, ν_0 is the frequency of attempts before an adatom can leave the surface, and J (monolayers s^{-1}) is the rate of impingement of CH_3 radicals from the gas phase to the substrate. The first term in Eq. (15) is derived from the volume energy of the cluster, whereas the second term is derived from the surface energy of the cluster. From the kinetic theory of gases, the rate of impingement of CH_3 radicals, J, can be derived as

$$J = \frac{N_A P_{\mathrm{HC}}}{\sqrt{2\pi MRT_g}} = 3.513\times 10^{22}\,\frac{P_{\mathrm{HC}}}{\sqrt{MT_g}}, \tag{16}$$

assuming that the molecules of the gas have a Boltzmann velocity distribution.[46] In Eq. (16), J is in $\mathrm{cm}^{-2}\ \mathrm{s}^{-1}$, N_A is Avogadro's number, P_{HC} is the partial pressure of the hydrocarbon species above the substrate surface in Torr, M is the molecular weight of the gas species in $g\ \mathrm{mol}^{-1}$, R is the gas constant, and T_g is the temperature in K of the gas mixture adjacent to the substrate surface.

In the present calculations, the deposition conditions typical of a direct current arcjet plasma assisted CVD system are used, as summarized in Table III. For the deposition conditions,[46] the impingement rate of CH_3 radicals (J) is calculated to be $1.8\times 10^{18}\ \mathrm{cm}^{-2}\ \mathrm{s}^{-1}$. The range of the characteristic frequencies for metal-CH_3 bonds is 2800–2900 cm^{-1}.[48] This frequency range corresponds to 8.4×10^{13}–$8.7\times 10^{13}\ \mathrm{s}^{-1}$. In this calculation, the value $\nu_0 = 8.55\times 10^{13}\ \mathrm{s}^{-1}$ is used. It has been reported elsewhere that typical values of ν_0 for a solid surface are in the range of 10^{13},[45] so the value used here is considered reasonable. When the data are substituted into the first term of Eq. (15), the result is

$$G_n = 3.85\times 10^{-12} n - (E_n + nE_a) \quad \text{(erg/molecule)}. \tag{17}$$

The surface energy contribution to G_n is computed using the heat of reaction for each of the elementary reactions constituting the CH_3 nucleation mechanisms. In this approach, the analysis of the clusters' stability is done not only from an energetic standpoint but also on entropic grounds because energetically and entropically favorable paths are only considered for the formation of the clusters. In order to calculate the surface energy, the cluster is assumed to be built by CH_3 radicals alone, as described in path 1 and path 2 as shown in Fig. 3, since paths 1 and 2 in Fig. 3 are the only energetically and entropically favorable pathways among the paths studied in this work leading to the nucleation of hydrogenated carbon clusters. In the following, the surface energy and therefore, the CCS is computed, for the two different paths of the proposed nucleation mechanism in Fig. 3.

TABLE III. Deposition parameters used in calculations.[a]

Total gas pressure	30 Torr
Gas composition at the exit of a plasma arc-jet	1.1% CH_4, 14.3% H, 84.6% H_2
Gas temperature above substrate surface	1200 K
Mole fraction of CH_3 radicals above substrate surface	2×10^{-4}
Substrate temperature	1133 K

[a]Reference 47.

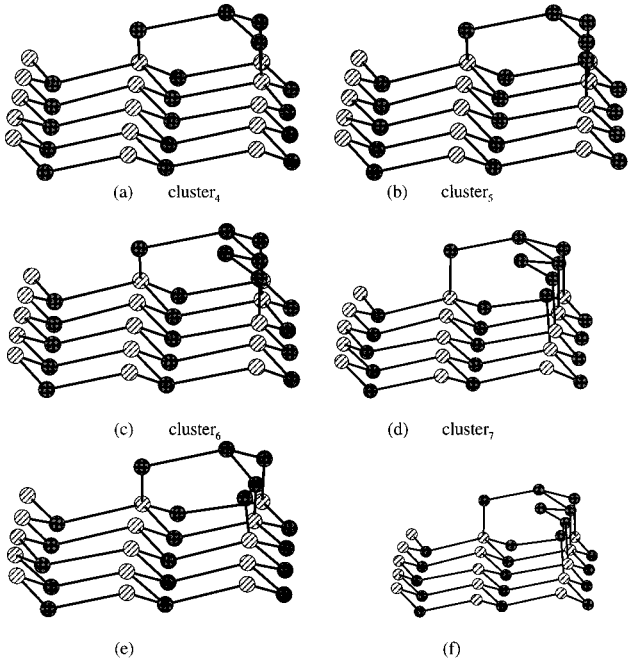

FIG. 4. Clusters containing different number of carbon atoms in reference to case I for determination of CCS. H atoms are not given in figure. (●): C atom, (⊘): Si atom. Bond lengths not to scale.

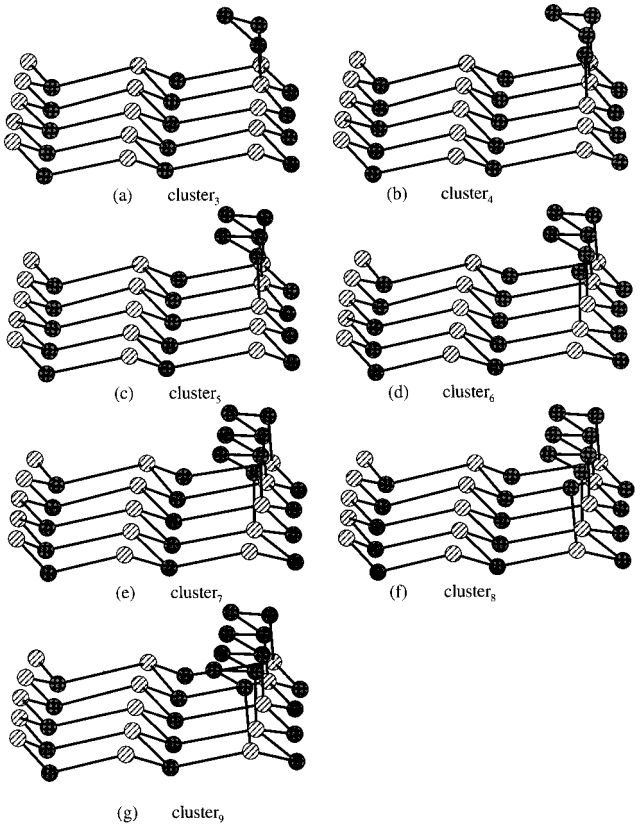

FIG. 5. Clusters containing different number of carbon atoms in reference to case II for determination of CCS. H atoms are not given in figure. (●): C atom, (⊘): Si atom. Bond lengths not to scale.

CH_3: NUCLEATION PRECURSOR

It is clear that the number of possible cluster structures increases with the number of CH_3 radicals incorporated into the cluster. For illustrative purposes, two different paths of cluster formation using CH_3 are investigated. The two cases (case I and case II) represent different sites of CH_3 adsorption, leading to different cluster structure. In case I, the adatoms are adsorbed on sites in adjacent silicon atom rows of the β-SiC(111) surface whereas, in case II, the CH_3 radicals are adsorbed on silicon atom sites in the same row.

Clusters of n carbon atoms with $n>3$, for cases I and II are shown in Figs. 4 and 5, respectively. Clusters with $n\leqslant 3$ are presented in Fig. 3. The cluster is in the shape of a puckered monolayer disk. This shape of clusters has been suggested based on theoretical work[49] and subsequently observed by a number of investigators experimentally.[50]

The elementary steps required to form the clusters of different sizes are not shown in Figs. 4 and 5 but are instead represented in the reactions shown in Table IV. The heat of reaction (in kcal/mol) at 1200 K is listed in the table with each reaction. The Gibbs energy change of each reaction has been calculated and is negative for all reactions in each sequence. The surface energy term, E_n+nE_a, for each cluster is listed with the final reaction for that cluster (identified by S_n) representing the formation of the cluster of size n. The reactions are identified as follows: $[EL_{nj}]$ is the jth elementary reaction during the formation of cluster of size n, $[EH_n]$ is the heat of reaction for the formation of hydrogen atoms, $[\mathrm{ET}_n]$ is the sum of the elementary reactions to form n sized cluster, that is,

$$[\mathrm{ET}_n]=\sum_{k=1}^{n}\sum_{j}\mathrm{EL}_{kj}, \tag{18}$$

and $[S_n]$ is the sum of $[\mathrm{ET}_n]$ and $[\mathrm{EH}_n]$. The quantity $[S_n]$ represents the sum of the binding energy and the adsorption energy of carbon clusters of size n on the substrate.

Case I: While Fig. 3 depicts the formation of clusters up to three carbon atoms, clusters containing more than three carbon atoms are shown in Fig. 4. A cluster of one carbon atom is shown in Fig. 3(a), two carbon atoms in Fig. 3(b), and three carbon atoms shown in Fig. 3(c). Clusters in Figs. 4(e) and 4(f) are not predicted to form because they are not energetically and entropically feasible. The elementary reactions leading to the formation of clusters illustrated in Figs. 4(a)–4(d) are listed in Table IV. Path 1 in Fig. 3 which forms a propane-like kernel is represented by the elementary reactions shown in Table IV. Path 2 is not represented in terms of elementary reactions in a separate table because it has already been listed in the text. Moreover, path 2 is already illustrated in Fig. 3. It is to be noted that the propane-like kernel can form by the two different paths, path 1 and path 2, but clusters containing more than three atoms follow the same path as listed in Table IV. While calculating the Gibbs energies for the propane-like kernel by path 2, the ΔH for each elementary reaction listed in Fig. 3 is utilized.

Case II: Clusters containing more than three carbon atoms are shown in Fig. 5. A cluster of one carbon atom is shown in Fig. 3(a), two atoms in Fig. 3(b), and three carbon atoms in Fig. 3(c). The elementary reactions required to form clusters of more than three atoms are listed in V. The elementary steps required to form clusters of up to three carbon atoms by path 1 are the same as reported for case I, hence they are not listed in Table V. The elementary reactions for the formation of the propane-like kernel by path 2

TABLE IV. Elementary reactions for the formation of clusters as described in Case I.

Reaction	ΔH_{1200} (kcal/mol)	Reaction name
$SiH(s)+H \Leftrightarrow Si\cdot(s)+H_2$	−37.247	EL_{11}
$Si\cdot(s)+CH_3 \Leftrightarrow SiCH_3(s)$	−66.213	EL_{12}
$SiH(s)+H+CH_3 \Leftrightarrow SiCH_3(s)+H_2$	−103.46	ET_1
$H_2 \Leftrightarrow 2H$	106.36	EH_1
$SiH(s)+CH_3 \Leftrightarrow SiCH_3(s)+H$	2.9	$S_1=E_1+E_a$
$SiH(s)+H \Leftrightarrow Si\cdot(s)+H_2$	−37.247	EL_{21}
$Si\cdot(s)+CH_3 \Leftrightarrow SiCH_3(s)$	−70.193	EL_{22}
$SiCH_3(s)+H \Leftrightarrow SiCH_2\cdot(s)+H_2$	−22.16	EL_{23}
$SiCH_3(s)+H \Leftrightarrow SiCH_2\cdot(s)+H_2$	−20.59	EL_{24}
$SiCH_2\cdot(s)+SiCH_2\cdot(s) \Leftrightarrow SiCH_2CH_2Si(s)$	−39.47	EL_{25}
$2SiH(s)+4H+2CH_3 \Leftrightarrow SiCH_2CH_2Si(s)+4H_2$	−293.12	ET_2
$4H_2 \Leftrightarrow 8H$	425.44	EH_2
$2SiH(s)+2CH_3 \Leftrightarrow SiCH_2CH_2Si(s)+4H$	132.32	$S_2=E_2+2E_a$
$SiCH_2CH_2Si(s)+H(g) \Leftrightarrow SiCH_2\cdot(s)+SiCH_3(s)$	−46.48	EL_{31}
$SiCH_2\cdot(s)+SiCH_3(s)+CH_3 \Leftrightarrow SiCH_2CH_3(s)+SiCH_3(s)$	−61.53	EL_{32}
$SiCH_2CH_3(s)+SiCH_3(s)+H \Leftrightarrow SiCH_2CH_2\cdot(s)+SiCH_3(s)+H_2$	−11.46	EL_{33}
$SiCH_2CH_2\cdot(s)+SiCH_3(s)+H \Leftrightarrow SiCH_2\cdot(s)+SiCH_2CH_2\cdot(s)+H_2$	−6.72	EL_{34}
$SiCH_2\cdot(s)+SiCH_2CH_2\cdot(s) \Leftrightarrow SiCH_2CH_2CH_2Si(s)$	−76.225	EL_{35}
$2SiH(s)+7H+3CH_3 \Leftrightarrow SiCH_2CH_2CH_2Si(s)+6H_2$	−495.535	ET_3
$6H_2 \Leftrightarrow 12H$	638.16	EH_3
$2SiH(s)+3CH_3 \Leftrightarrow SiCH_2CH_2CH_2Si(s)+5H$	142.625	$S_3=E_3+3E_a$
$SiH(s)+H \Leftrightarrow Si\cdot(s)+H_2$	−37.247	EL_{41}
$Si\cdot(s)+CH_3 \Leftrightarrow SiCH_3(s)$	−68.478	EL_{42}
$SiCH_3(s)+H \Leftrightarrow SiCH_2\cdot(s)+H_2$	−22.16	EL_{43}
$SiCH_2CH_2CH_2Si(s)+H \Leftrightarrow SiCH_2CH\cdot CH_2Si(s)+H_2$	−3.42	EL_{44}
$SiCH_2CH\cdot CH_2Si(s)+SiCH_2\cdot(s) \Leftrightarrow cluster_4(s)$	−72.98	EL_{45}
$3SiH(s)+4CH_3+10H \Leftrightarrow cluster_4(s)+9H_2$	−699.82	ET_4
$9H_2 \Leftrightarrow 18H$	957.24	EH_4
$3SiH(s)+4CH_3 \Leftrightarrow cluster_4(s)+8H$	257.42	$S_4=E_4+4E_a$
$SiH(s)+H \Leftrightarrow Si\cdot(s)+H_2$	−37.247	EL_{51}
$Si\cdot(s)+CH_3 \Leftrightarrow SiCH_3(s)$	−69.033	EL_{52}
$4SiH(s)+5CH_3+11H \Leftrightarrow cluster_5(s)+10H_2$	−806.1	ET_5
$10H_2 \Leftrightarrow 20H$	1063.6	EH_5
$4Si(s)+5CH_3 \Leftrightarrow cluster_5(s)+9H$	257.5	$S_5=E_5+5E_a$
$SiCH_3(s)+H \Leftrightarrow SiCH_2\cdot(s)+H_2$	−22.12	EL_{61}
$SiCH_2\cdot(s)+CH_3 \Leftrightarrow SiCH_2CH_3(s)$	−61.98	EL_{62}
$SiCH_2CH_3(s)+H \Leftrightarrow SiCH_2CH_2\cdot(s)+H_2$	−12.11	EL_{63}
$cluster_5(s)+H \Leftrightarrow cluster_5\cdot(s)+H_2$	−7.86	EL_{64}
$cluster_5\cdot(s)+SiCH_2CH_2\cdot(s) \Leftrightarrow cluster_6(s)$	−68.82	EL_{65}
$4SiH(s)+6CH_3+14H \Leftrightarrow cluster_6(s)+13H_2$	−978.99	ET_6
$13H_2 \Leftrightarrow 26H$	1382.68	EH_6
$4SiH(s)+6CH_3 \Leftrightarrow cluster_6(s)+12H$	403.69	$S_6=E_6+6E_a$
$SiH(s)+H \Leftrightarrow Si\cdot(s)+H_2$	−37.247	EL_{71}
$Si\cdot(s)+CH_3 \Leftrightarrow SiCH_3(s)$	−69.203	EL_{72}
$5SiH(s)+7CH_3+15H \Leftrightarrow cluster_7(s)+14H_2$	−1085.44	ET_7
$14H_2 \Leftrightarrow 28H$	1489.04	EH_7
$5SiH(s)+7CH_3 \Leftrightarrow cluster_7(s)+13H_2$	403.6	$S_7=E_7+7E_a$

are not listed separately in a table for the same reasons stated in case I.

RESULTS OF CRITICAL CLUSTER SIZE CALCULATIONS

Case I results: The Gibbs energy of formation of clusters up to seven carbon atoms calculated using Eq. (17) are given in Table VI for path 1 and path 2 for case I. The Gibbs energy of formation of clusters consisting of more than five carbon atoms is negative for both path 1 and path 2, which means that such clusters are stable and do not dissociate. Therefore, the CCS for the cluster formation shown in Fig. 4 is 5.

Case II results: The Gibbs energy of formation of clusters (shown in Fig. 5) of size up to 10 carbon atoms is given in Table VI for case II for both paths 1 and 2. The CCS in this case is eight carbon atoms because the Gibbs energy of clusters of size greater than 8 is negative, indicating that the clusters containing more than eight carbon atoms are stable.

Therefore, the CCS calculated is either five or eight depending on the type of site at which the CH_3 precursor ad-

TABLE V. Elementary reactions for the formation of clusters as described in Case II.

Reaction	ΔH_{1200} (kcal/mol)	Reaction name
$SiH(s)+H \Leftrightarrow Si\cdot(s)+H_2$	−37.247	EL_{41}
$Si\cdot(s)+CH_3 \Leftrightarrow SiCH_3(s)$	−69.203	EL_{42}
$3SiH(s)+4CH_3+8H \Leftrightarrow Si(CH_2)_3Si(s)+SiCH_3(s)+7H_2$	−601.99	ET_4
$7H_2 \Leftrightarrow 14H$	744.52	EH_4
$3SiH(s)+4CH_3 \Leftrightarrow Si(CH_2)_3Si(s)+SiCH_3(s)+6H$	142.53	$S_4=E_4+4E_a$
$SiCH_3(s)+H \Leftrightarrow SiCH_2\cdot(s)+H_2$	−21.99	EL_{51}
$SiCH_2\cdot(s)+CH_3 \Leftrightarrow SiCH_2CH_3(s)$	−61.85	EL_{52}
$SiCH_2CH_3(s)+H \Leftrightarrow SiCH_2CH_2\cdot(s)+H_2$	−12.33	EL_{53}
$SiCH_2CH_2CH_2Si(s)+H \Leftrightarrow SiCH_2CH_2CH\cdot Si(s)+H_2$	−12.58	EL_{54}
$SiCH_2CH_2CH\cdot Si(s)+SiCH_2CH_2\cdot(s) \Leftrightarrow cluster_5(s)$	−68.06	EL_{55}
$3SiH(s)+5CH_3+11H \Leftrightarrow cluster_5(s)+10H_2$	−778.8	ET_5
$10H_2 \Leftrightarrow 20H$	1063.6	EH_5
$3SiH(s)+5CH_3 \Leftrightarrow cluster_5(s)+9H$	284.8	$S_5=E_5+5E_a$
$SiH(s)+H \Leftrightarrow Si\cdot(s)+H_2$	−37.247	EL_{61}
$Si\cdot(s)+CH_3 \Leftrightarrow SiCH_3(s)$	−68.903	EL_{62}
$4SiH(s)+6CH_3+12H \Leftrightarrow cluster_6(s)+11H_2$	−884.95	ET_6
$11H_2 \Leftrightarrow 22H$	1169.96	EH_6
$4SiH(s)+6CH_3 \Leftrightarrow cluster_6(s)+10H$	285.01	$S_6=E_6+6E_a$
$SiCH_3(s)+H \Leftrightarrow SiCH_2\cdot(s)+H_2$	−21.99	EL_{71}
$SiCH_2\cdot(s)+CH_3 \Leftrightarrow SiCH_2CH_3(s)$	−61.85	EL_{72}
$SiCH_2CH_3(s)+H \Leftrightarrow SiCH_2CH_2\cdot(s)+H_2$	−12.31	EL_{73}
$cluster_5(s)+H \Leftrightarrow cluster_5\cdot(s)+H_2$	−11.98	EL_{74}
$cluster_5\cdot(s)+SiCH_2CH_2\cdot(s) \Leftrightarrow cluster_7(s)$	−68.06	EL_{75}
$4SiH(s)+7CH_3+15H \Leftrightarrow cluster_7(s)+14H_2$	−1061.14	ET_7
$14H_2 \Leftrightarrow 28H$	1489.04	EH_7
$4SiH(s)+7CH_3 \Leftrightarrow cluster_7(s)+13H$	427.9	$S_7=E_7+7E_a$
$SiH(s)+H \Leftrightarrow Si\cdot(s)+H_2$	−37.247	EL_{81}
$Si\cdot(s)+CH_3 \Leftrightarrow SiCH_3(s)$	−69.2	EL_{82}
$5SiH(s)+8CH_3+16H \Leftrightarrow cluster_8+15H_2$	−1167.587	ET_8
$15H_2 \Leftrightarrow 30H$	1595.4	EH_8
$5SiH(s)+8CH_3 \Leftrightarrow cluster_8(s)+14H$	427.813	$S_8=E_8+8E_a$
$SiCH_3(s)+H \Leftrightarrow SiCH_2\cdot(s)+H_2$	−21.98	EL_{91}
$SiCH_2\cdot(s)+CH_3 \Leftrightarrow SiCH_2CH_3(s)$	−61.863	EL_{92}
$SiCH_2CH_3(s)+H \Leftrightarrow SiCH_2CH_2\cdot(s)+H_2$	−12.31	EL_{93}
$cluster_7(s)+H \Leftrightarrow cluster_7\cdot(s)+H_2$	−11.98	EL_{94}
$cluster_7\cdot(s)+SiCH_2CH_2\cdot(s) \Leftrightarrow cluster_9(s)$	−68.06	EL_{95}
$5SiH(s)+9CH_3+19H \Leftrightarrow cluster_9(s)+18H_2$	−1343.78	ET_9
$18H_2 \Leftrightarrow 36H$	1914.48	EH_9
$5SiH(s)+9CH_3 \Leftrightarrow cluster_9(s)+17H$	570.7	$S_9=E_9+9E_a$
$SiH(s)+H \Leftrightarrow Si\cdot(s)+H_2$	−37.247	EL_{101}
$Si\cdot(s)+CH_3 \Leftrightarrow SiCH_3(s)$	−68.9	EL_{102}
$6SiH(s)+20H+10CH_3 \Leftrightarrow cluster_{10}(s)+19H_2$	−1449.927	ET_{10}
$19H_2 \Leftrightarrow 38H$	2020.84	EH_{10}
$6SiH(s)+10CH_3 \Leftrightarrow cluster_{10}(s)+18H$	570.913	$S_{10}=E_{10}+10E_a$

sorbs. It is important to note that the desorption of the entire cluster has not been considered in this work. Had the desorption of the cluster been considered, the CCS would undoubtedly have been more than that predicted in this work. The computed critical nucleus size agrees well with the experimental data and theoretical results reported in the literature.[51,52] The CCS computed here is smaller than the computer simulation results,[53,54] simply because desorption of the entire cluster has not been considered in this work. These etch resistant and stable nanometer scale diamond crystallites could serve as nucleation seeds by providing high surface free energy sites for diamond nucleation.

SUMMARY

A possible model for the nucleation mechanism of diamond phase carbon clusters on the β-SiC(111) surface, which forms epitaxially on Si(111) substrates, is presented. Several mechanistic pathways are examined, including (1) the formation of clusters from CH_3 radicals alone, and (2) the formation of clusters with C_2H_2 and CH_3 as nucleation precursors. A molecular mechanics approach is utilized to predict an entropically and energetically favorable pathway for diamond nucleation. A CH_3 based nucleation route involving radical-radical surface reactions is proposed as a favorable

TABLE VI. Gibbs energy of clusters at 1133 K substrate temperature.

Gibbs energy, G_n ($10^{12}\times$ergs)	CH_3: case I path 1	CH_3: case I path 2	CH_3: case II path 1	CH_3: case II path 2
G_1	3.646	3.646	3.646	3.646
G_2	−1.533	7.569	−1.533	7.569
G_3	1.595	1.585	1.595	1.585
G_4	−2.563	−2.572	5.448	5.440
G_5	1.278	1.270	−0.626	−0.633
G_6	−5.069	−5.076	3.206	3.199
G_7	−1.216	−1.222	−2.911	−2.917
G_8	---	---	0.942	0.937
G_9	---	---	−5.175	−5.179
G_{10}	---	---	−1.343	−1.346

route for nucleation of diamond phase carbon clusters. The proposed nucleation mechanism using CH_3 radicals is both energetically and entropically feasible. This mechanism may explain the incubation period observed during the early stages of nucleation and growth of diamond due to the steric selectivity inherent to the mechanism, thereby lowering the nucleation rate. A large negative entropy change in elementary reactions in the proposed C_2H_2 and CH_3 mechanisms prevents the nucleation of diamond-phase carbon clusters. The critical cluster size for diamond-phase clusters is computed based on the atomistic theory of nucleation. The critical cluster size is calculated based on the proposed and feasible nucleation mechanism using CH_3 alone as the nucleation precursor. The CCS is computed to be in the nanometer scale. However, the CCS calculated in this work is based on the assumption that entire clusters do not desorb from the substrates resulting in the prediction of smaller critical clusters in this work as compared to the CCS prediction by others when the desorption of entire clusters had been considered. Clusters greater than CCS are stable because of their negative free energy of formation. It is proposed that these diamond nanocrystallites may serve as nucleation centers or seeds for diamond nucleation. It may be speculated from the oscillatory behavior of G_n vs n, that clusters of size n such that $G_n<0$, $G_{n-1}>0$, and $G_{n+1}>0$, could be trapped in the diamond matrix because it would be unfavorable for such clusters to either grow or dissociate due to the positive free energy of formation of clusters of size $n+1$ and $n-1$, respectively.

ACKNOWLEDGMENTS

This work has been supported by the Materials Science Program at DARPA, Contract N00014-93-1-2002, and through partial support by Texas Instruments. P.M. would like to thank Dr. Georgia McGaughey for her help with MM3.

[1] H. Liu and D. S. Dandy, Diamond Chemical Vapor Deposition, Nucleation and Growth Stages (Noyes, Park Ridge, NJ, 1995).
[2] X. Jiang, K. Schiffmann, A. Westphal, and C.-P. Klages, Appl. Phys. Lett. **63**, 1203 (1993); X Jiang, K. Schiffmann, and C. P. Klages, Phys. Rev. B **50**, 8402 (1994).
[3] K. Tamaki, Y. Watanabe, Y. Nakamura, and S. Hirayama, Thin Solid Films **236**, 115 (1993).
[4] D. Kim, H. Lee, and J. Lee, J. Mater. Sci. **28**, 6704 (1993).
[5] M. Frenklanch, W. Howard, D. Huang, J. Yuan, K. E. Spear, and R. Koba, Appl. Phys. Lett. **59**, 546 (1991).
[6] P. Bou, L. Vandelbulcke, R. Herbin, and F. Hillion, J. Mater. Res. **7**, 2151 (1992).
[7] W. R. L. Lambrecht, C. H. Lee, B. Segall, and J. C. Angus, etc., Nature (London) **364**, 607 (1993).
[8] J. J. Dubray, C. G. Pantano, M. Melocelli, and E. Bertran, J. Vac. Sci. Technol. A **9**, 3012 (1991).
[9] J. Narayan, V. P. Godbole, G. Matera, and R. K. Singh, J. Appl. Phys. **71**, 966 (1992).
[10] C. P. Sung and H. C. Shih, J. Mater. Res. **7**, 105 (1992).
[11] A. A. Morrish and P. E. Pehrsson, Appl. Phys. Lett. **59**, 417 (1991).
[12] R. Meilunas, M. S. Wong, K. C. Sheng, and R. P. H. Chang, Appl. Phys. Lett. **54**, 2204 (1989).
[13] A. R. Badzian and T. Badzian, Surf. Coat. Technol. **36**, 283 (1988).
[14] K. F. Turner, B. R. Stoner, L. Bergman, J. T. Glass, and R. J. Nemanich, J. Appl. Phys. **69**, 6400 (1991).
[15] D. N. Belton, S. J. Harris, S. J. Schmieg, A. M. Weiner, and T. A. Perry, Appl. Phys. Lett. **54**, 416 (1989).
[16] K. Kobayashi, S. Karasawa, T. Watanabe, and F. Togashi, J. Cryst. Growth **99**, 1211 (1990).
[17] P. O. Joffreau, R. Haubner, and B. Lux, Int. J. Refract. Hard Met. **7**, 186 (1988).
[18] R. A. Rudder, G. C. Hudson, R. C. Hendry, R. E. Thomas, J. B. Posthill, and R. J. Markunas, *Proceedings of the First International Conference on the Applications of Diamond Films and Related Materials*, edited by Y. Tzeng, M. Yoshikawa, M. Murakawa, and A. Feldman, (Elsevier, New York, 1991), p. 395.
[19] K. V. Ravi and C. A. Koch, Appl. Phys. Lett. **57**, 348 (1990).
[20] B. R. Stoner, G.-H. M. Ma, S. D. Wolter, and J. T. Glass, Phys. Rev. B **45**, 11067 (1992).
[21] S. P. McGinnis, M. A. Kelly, T. M. Gun, and S. B. Hagstrom, *Proceedings of the Third Symposium on Diamond and Related Materials*, edited by Dismukes and Ravi (Electrochemical Society, Pennington, NJ, 1993), p. 153.
[22] P. Badziag, W. Verwoerd, W. Ellis, and N. Greiner, Nature **343**, 244 (1990).
[23] M. A. George, A. Burger, W. E. Collins, J. L. Davidson, A. V. Barnes, and N. H. Tolk, J. Appl. Phys. **76**, 4099 (1994).
[24] B. E. Williams, J. T. Glass, and R. F. Davis, J. Cryst. Growth **99**, 1168 (1990); B. E. Williams and J. T. Glass, J. Mater. Res. **4**, 373 (1989).
[25] N. Jiang, B. W. Sun, Z. Zhang, and Z. Lin, J. Mater. Res. **9**, 2695 (1994).
[26] B. R. Stoner, S. R. Sahaida, and J. P. Bade, etc., J. Mater. Res. **8**, 1334 (1993).
[27] U. Burkert and N. L. Allinger, Molecular Mechanics (American Chemical Society, Washington, DC, 1982).
[28] N. L. Allinger and J. Li, J. Am. Chem. Soc. **111**, 8551 (1989); J. Li and N. L. Allinger, J. Am. Chem. Soc. **111**, 8576 (1989); N. L. Allinger, F. Li, and L. Yan, J. Comput. Chem. **11**, 849 (1990); N. L. Allinger, F. Li, L. Yan, and J. C. Tai, J. Comput. Chem. **11**, 868 (1990).
[29] MM3(92) Operation Manual, *Quantum Chemistry Program Exchange* (University of Indiana, Bloomington, IN, 1989).
[30] E. A. Brandes, Smithells Metals Reference Book, 6th ed. (Butterworth, London, 1983).
[31] S. J. Harris, Appl. Phys. Lett. **56**, 2298 (1990).
[32] F. G. Celii, P. E. Pehrrson, H. T. Wang, and J. E. Bulter, Appl. Phys. Lett. **52**, 2043 (1988).
[33] Y. Ohshita, J. Cryst. Growth **110**, 516 (1991).
[34] J. C. Angus and C. C. Hayman, Science **241**, 913 (1988).
[35] Y. Matsui, H. Yabe, and Y. Hirose, Jpn. J. Appl. Phys. 1 **29**, 1552 (1990).
[36] I. Barin, Thermochemical Data of Pure Substances, (VCH, New York, 1993), Part I.
[37] K. Hermann and P. S. Bagus, Phys. Rev. B **20**, 1603 (1979).
[38] D. D. Wagman, W. H. Evans, V. B. Parker, R. H. Schumm, I. Halow, S. M. Bailey, K. L. Churney, and R. L. Nuttall, J. Phys. Chem. Ref. Data **11**, Suppl. No. 2 (1982).
[39] M. Frenklach and K. E. Spear, J. Mater. Res. **3**, 133 (1988).
[40] D. Huang, M. Frenklach, and M. Maroncelli, J. Phys. Chem. **92**, 6379 (1988).
[41] D. Huang and M. Frenklach, J. Phys. Chem. **95**, 3692 (1991).
[42] M. Frenklach and H. Wang, Phys. Rev. B **43**, 1520 (1991).
[43] S. J. Harris and D. N. Belton, Jpn. J. Appl. Phys. 1 **30**, 2615 (1991).
[44] J. L. Kenty and J. P. Hirth, Trans. Metall. Soc. AIME **245**, 2373 (1969).

[45] B. Lewis and J. C. Anderson, Nucleation and Growth of Thin Films (Academic, London, 1978), Chaps. 4, 5, and 9.
[46] H. Liu, and D. S. Dandy, J. Electrochem. Soc. **143**, 1104 (1995).
[47] M. E. Coltrin and D. S. Dandy, J. Appl. Phys. **74**, 5803 (1993).
[48] L. H. Little, Infrared Spectra of Adsorbed Species (Academic, London, 1966), Chap. 5.
[49] E. Molinari, R. Polini, and M. Tomellini, J. Mater. Res. **8**, 798 (1993).
[50] J. Singh, J. Mater. Sci. **29**, 2761 (1994).
[51] S. Yugo, A. Izumi, T. Kanai, T. Muto, and T. Kimura, *New Diamond Science* Technology, edited by R. Messier, J. T. Glass, J. E. Butler, and R. Roy (MRS, Pittsburgh, PA, 1991), p. 385; S. Yugo, T. Kanai, and T. Kimura, Diam. Relat. Mater. **1**, 929 (1992).
[52] M. Tomellini, Ber. Bunsenges. Phys. Chem. **99**, 838 (1995).
[53] J. C. Angus, M. Sunkara, S. R. Sahaida, and J. T. Glass, J. Mater. Res. **7**, 3001 (1992).
[54] M. Sunkara, Ph.D. thesis, Case Western Reserve University, 1993.